Article ID: 1000-324X(2022)01-0101-06 **DOI:** 10.15541/jim20200653

Metal Sulfide Ag_2S: Fabrication *via* Zone Melting Method and Its Thermoelectric Property

JIN Min[1], BAI Xudong[2], ZHANG Rulin[1], ZHOU Lina[1], LI Rongbin[1]

(1. School of Materials Science, Shanghai Dianji University, Shanghai 201306, China; 2. School of Materials Science and Engineering, University of Shanghai for Science and Technology, Shanghai 200093, China)

Abstract: Metal sulfide Ag_2S is an attractive semiconductor due to its excellent physical and chemical property that enable it with wide applications in fields of catalysis, sensing, optoelectronics in past years. In present work, ϕ18 mm× 50 mm Ag_2S ingot was successfully prepared using zone melting method and its thermoelectric (TE) behavior was investigated. Ag_2S has standard monoclinic $P2_1/c$ space group (α-Ag_2S phase) below 450 K and transfer to cubic structure (β-Ag_2S phase) over this temperature. Ag_2S is a *n*-type semiconductor as the Seebeck coefficient *S* is always negative due to the Ag interstitial ions in the material that can provide additional electrons. *S* is about −1200 $\mu V \cdot K^{-1}$ near room temperature, declines to −680 $\mu V \cdot K^{-1}$ at 440 K and finally decreases to ~−100 $\mu V \cdot K^{-1}$ at β-Ag_2S state. The electrical conductivity (σ) of α-Ag_2S is almost zero. However, the value sharply jumps to ~40000.5 $S \cdot m^{-1}$ as the material just changes to β-Ag_2S at 450 K and then gradually deceases to 33256.2 $S \cdot m^{-1}$ at 650 K. Hall measurement demonstrates that carrier concentration n_H of Ag_2S is suddenly increased from the level of ~10^{17} cm^{-3} to ~10^{18} cm^{-3} during phase transition. Total thermal conductivity κ of α-Ag_2S is ~0.20 $W \cdot m^{-1} \cdot K^{-1}$ but is ~0.45 $W \cdot m^{-1} \cdot K^{-1}$ of β-Ag_2S. Ultimately, a maximum ZT=0.57 is achieved around 580 K that means Ag_2S might be a promising middle-temperature TE material.

Key words: Ag_2S; zone melting; thermoelectric material; phase transition

During the past years, metal sulfide Ag_2S has attracted much attention due to its excellent physical and chemical properties that enable it with various applications in fields of catalysis, sensing, optoelectronics and so on[1–6]. For example, Dong, *et al*[7] reports Ag_2S-nanowire is an ideal candidate for making nano temperature and photoelectric sensors as its photoconductivity is always positive under 532 or 1064 nm laser radiation. Du, *et al*[8] declares Ag_2S Quantum Dots may act as nontoxic carrier for potential *in vivo* bioimaging. Zhang, *et al*[9] confirms that the Ag_2S Quantum Dots indeed open up the possibility of *in vivo* anatomical imaging and early stage tumor diagnosis owing to their high emission efficiency in NIR-II imaging window. Besides, Ag_2S is also found suitable for solar cell and infrared sensitivity device fabrication attribute to its semiconductor character which has a ~1.0 eV band gap[10]. Recently, it is announced that Ag_2S exhibits a fantastic room-temperature ductile behavior. Its compression deformation can reach 50%, the bending variable surpassing 20%, and the stretching variable up to 4.2%. These shape variables are far more than known ceramic and semiconductor materials, and are equivalent to the mechanical properties of some metals. Consequently, Ag_2S provides a possibility is quest of producible inorganic semiconductors/ceramics for flexible electronic devices[11].

In order to develop more interesting functions of Ag_2S, the authors focus on its potential thermoelectric (TE) behavior according to the concept of Seebeck-Peltier effect[12]. The TE device can supply green and reliable energy by direct conversion of heat into electricity. Thus, it is expected to have wide applications in power generation. The efficiency of a thermoelectric material is usually evaluated by the dimensionless figure of merit ZT, $ZT = (S^2T\sigma)/\kappa$. Where S is Seebeck coefficient, T is absolute temperature, σ is electrical conductivity and κ is thermal conductivity[13]. From the view of this formula, it is obvious that the TE material with ultra-low thermal conductivity is one of a significant factor for high ZT. Based on this recognition, the TE behavior of Ag_2S is

Received date: 2020-11-16; **Revised date:** 2020-12-03; **Published online:** 2021-03-01
Foundation item: Shanghai Natural Science Foundation (19ZR1419900)
Biography: JIN Min (1982–), male, professor. E-mail: jmaish@aliyun.com
金 敏(1982–), 男, 教授. E-mail: jmaish@aliyun.com

worthy of study as it has very small thermal conductivity. Wang, *et al*[14] have fabricated Ag_2S ceramic using a solution method and the thermal transport analysis indicates that its total thermal conductivity is 0.4–0.6 $W·m^{-1}·K^{-1}$ in range of 300–600 K, which is lower than most solid TE materials. Ultimately, a maximum ZT=0.55 (580 K) is obtained which implies that Ag_2S is a promising middle-temperature TE material. In present work, a zone melting method which has the advantage of purifying materials is introduced for Ag_2S compound fabrication. Its electrical/thermal transport properties are systematically investigated and the final figure of merit ZT is demonstrated.

1 Experimental

1.1 Ag_2S preparation

99.999% high purity Ag and S elements were used as start materials for Ag_2S synthesis, they were weighed in accordance with the standard stoichiometric ratio and the total weight was about 60.5 g. The start materials were loaded into a ϕ18 mm quartz ampoule and then sealed with a vacuum less than 10^{-2} Pa, after that, the quartz ampoule was placed into a 1000 ℃ rocking furnace. After Ag and S totally melted, the rocking system worked at a rate of 20 r/min for 30 min to enhance Ag_2S synthesis homogeneity. Ultimately, Ag_2S compound was obtained as the furnace was cooled to room temperature naturally. Subsequently, the synthesized Ag_2S raw material with the same ampoule was put into a home-made zone melting furnace. The ampoule was supported by a Al_2O_3 pedestal and a pair of thermal-couples was installed near the bottom for temperature indication. Fig. 1(a) shows the schematic diagram of the zone melting furnace which was heated by a couple of Si-Mo heaters to form a narrow high temperature zone. Fig. 1(b) is the temperature profile along vertical direction, the temperature gradient for Ag_2S solidification was about 30–35 ℃/cm. The furnace temperature was controlled at 920 ℃. After Ag_2S raw material was melted, the quartz ampoule was lowered down at the speed of 3.0 mm/h until all solution was exhausted. The parameters for Ag_2S solidification are summarized in Table 1.

Table 1 Parameters for Ag_2S fabrication

Parameter	Zone melting
Weight of raw material/g	60.5
Quartz ampoule size/mm	ϕ18
Vacuum of quartz ampoule/Pa	$<10^{-2}$
Furnace temperature/℃	920
Temperature gradient/(℃·cm^{-1})	30–35
Lowering speed/(mm·h^{-1})	3.0

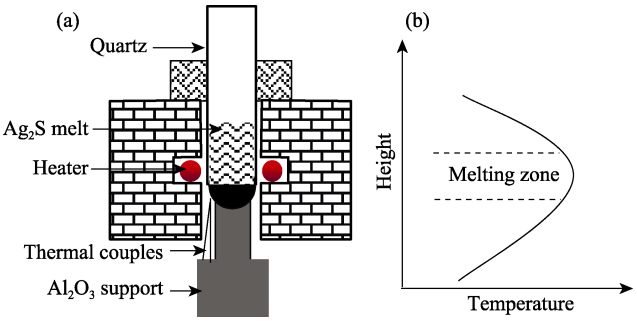

Fig. 1 Schematic diagram of the zone melting furnace (a) and temperature profile along vertical direction (b)

1.2 Characterization

The density ρ was measured by Archimedes principle. Phase structure of the material was analyzed by X-ray diffraction (XRD, Bruker D8, Germany) using Cu Kα radiation (λ=0.15406 nm) at room temperature. The morphological and chemical composition were investigated using Scanning Electron Microscope (SEM, JSM-6610, JEOL Ltd.) and Energy Dispersive Spectroscopy (EDS, JED-2300T) equipment. The Seebeck coefficient and electrical conductivity were measured simultaneously (ULVAC-RIKO ZEM-3) from 300 to 650 K. The thermal diffusivity D was tested by laser flash method (Netzsch, LFA-457, Germany). The total thermal conductivity κ was obtained using $\kappa=D·\rho·C_p$, where C_p is specific heat capacity.

2 Results and discussion

The as-grown Ag_2S ingot (ϕ18 mm× 50 mm) is easily separated from quartz ampoule and displays bright metallic luster, as Fig. 2 shows. Such phenomenon indicates that Ag_2S has none reaction with quartz ampoule during the whole process. Its density is measured to be 7.20 g/cm^3 that is nearly 100% close to the theoretical value 7.23 g/cm^3. Fig. 3(a) is the XRD pattern of Ag_2S powder, it is observed that all diffraction peaks are matched well to those of standard α-Ag_2S monoclinic $P2_1/c$ space group (PDF#14-0072) at room temperature. The lattice parameters a, b and c are calculated *via* a general structure analysis system, and the values are 0.4251, 0.6962 and 0.7873 nm, respectively. EDS measurement implies the atom percent of Ag is 67.2% and S is 32.8% in matrix that

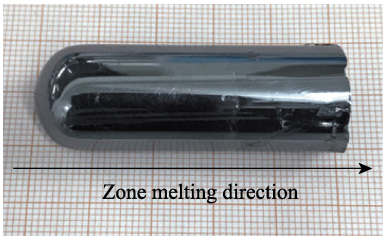

Fig. 2 Ag_2S ingot prepared by zone melting method

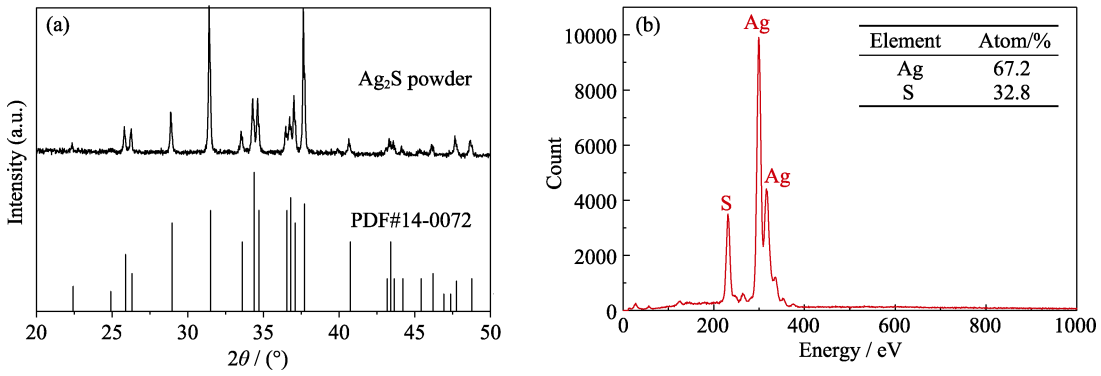

Fig. 3　XRD pattern (a) and EDS map (b) of Ag_2S

agrees well with the standard stoichiometric composition of Ag_2S, as Fig. 3(b) shows.

During SEM testing, it is interesting that some micro size particles oozed from the material. Fig. 4(a) shows the original Ag_2S surface under 25 kV voltage. However, in a very short time, numerous white particles came up and then gradually grew up for about 30 s, as Fig. 4(b,c) demonstrating. Thereafter, the particle sizes are kept stable. EDS analysis reveals the particle composition is 100% Ag. This result is mainly attributed to the special liquid-like character of Ag_2S. As previous literature[15] reported, Ag ions are weakly bonded to the neighbour atoms in silver chalcogenides Ag_2M (M=S, Se, Te) semiconductors, and apt to migrate from one site to another if there is sufficient energy force on them. For example, the external heat or voltage are both able to drive Ag ions movement. Therefore, it is easy to understand the high energy electron beam in SEM system plays a significant role causing the deposition of Ag. In fact, similar metal element deposition is also noticed in other type of liquid-like materials, such as Cu_2Se, Cu_2S, Ag_8SnSe_6 and so on[16–18].

As for thermoelectric property evaluation, sample 1# for electrical transport measurement is cut parallel to Ag_2S solidification direction, and sample 2# for thermal transport testing is processed along perpendicular orientation, as the insert in Fig. 5(a) shows. Here, we should note that such sample processing modes are widely adopted in other zone melting thermoelectric materials, such as Bi_2Te_3, SnSe, *etc*[19-20]. In Fig. 5(a), the relationship of temperature with Seebeck coefficient S is displayed. It is found that negative S that means Ag_2S is a *n*-type semiconductor. This conductive behavior might be due to the Ag interstitial ions in crystal structure that act as donor impurities providing additional electrons[14]. Near room temperature, S is about $-1200\ \mu V \cdot K^{-1}$. As the temperature increased to 440 K, S linearly deceased to $-680\ \mu V \cdot K^{-1}$. However, when temperature continuously increased to 450 K, S undergoes a sharp decline and the value is around $-100\ \mu V \cdot K^{-1}$. This dramatic change is mainly attributed to the phase transition of Ag_2S. Below 450 K, the material has an α-Ag_2S monoclinic structure. Nevertheless, it would transfer to β-Ag_2S body centered cubic structure as temperature surpasses 450 K. After that, S maintains a relative stable state regardless the increasing of temperature to 650 K. Fig. 5(b) shows the dependence of conductivity σ on temperature. It is amazing that the σ of α-Ag_2S is almost zero before 450 K. However, the σ value sharply jumps to ~40000.5 $S \cdot m^{-1}$ as the material just finishes phase transition. Then, σ gradually deceases to 33256.2 $S \cdot m^{-1}$ near 650 K. Fig. 5(c) exhibits power factor PF *vs* temperature that calculated from $PF = S^2\sigma$. It is observed that the PF of α-Ag_2S is much poor because of its weak conductive property. As for β-Ag_2S, PF is practically a constant ~6 $\mu W \cdot cm^{-1} \cdot K^{-2}$ in temperature range of 450–650 K.

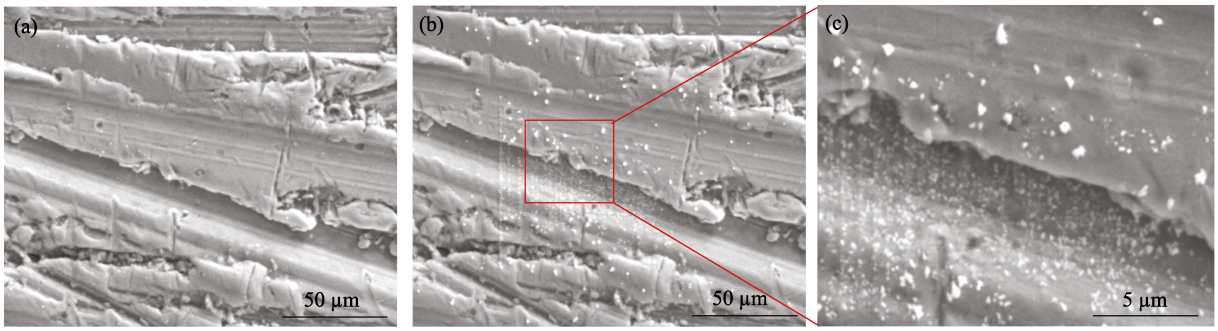

Fig. 4　SEM images of original Ag_2S surface (a), Ag particles on Ag_2S matrix (b) and enlarged morphology of the surface (c)

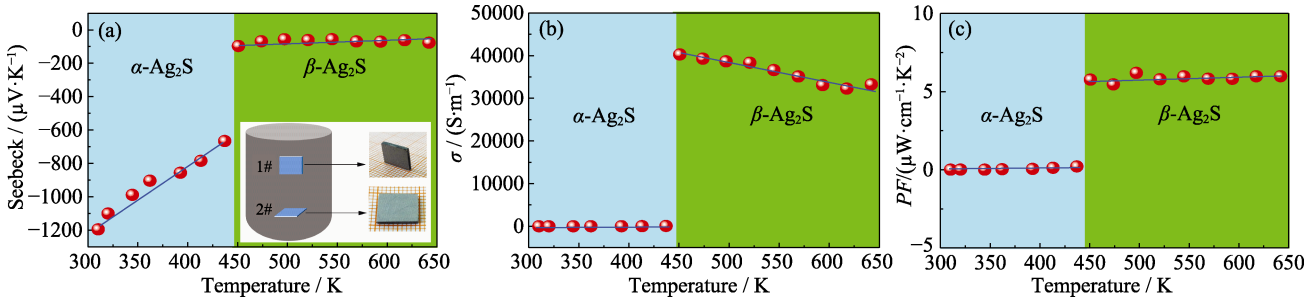

Fig. 5 Relationship of Seebeck (a), electrical conductivity σ (b) and power factor PF (c) with temperature

In order to better understand the electrical transport behavior of Ag_2S, the Hall properties are also characterized. Fig. 6(a) shows the temperature dependence of carrier concentration n_H. Near room temperature, the n_H value is on level of ~10^{17} cm^{-3}. Then, as temperature is increased to the threshold of phase transition, n_H is climbed to ~10^{18} cm^{-3}. This phenomenon is mainly due to the increase of carrier concentration from valence band to conduction band when temperature is added. As expected, when Ag_2S is transformed from monoclinic to body centered cubic structure, n_H is increased suddenly to ~10^{19} cm^{-3} near 450 K. Later, a growing number of carriers are generated in β-Ag_2S, and n_H rises to a highest ~10^{20} cm^{-3} level at 650 K. Fig. 6(b) is the carrier mobility μ_H diagram varied with temperature. Similar to carrier concentration, μ_H has a dramatic jump during phase transition. Besides, it is noticed μ_H is always declined when it is in α-Ag_2S and β-Ag_2S states, respectively. The maximum μ_H= 161.6 $cm^2 \cdot V^{-1} \cdot s^{-1}$ happens at the moment as Ag_2S finishes phase transition.

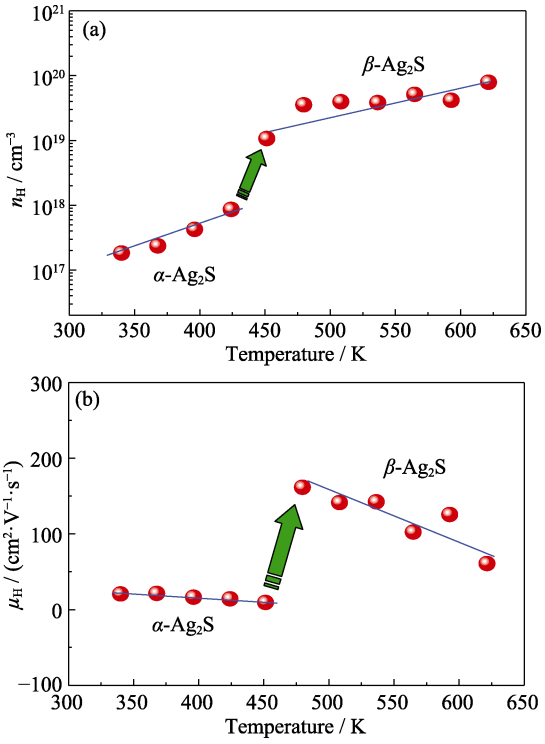

Fig. 6 Carrier concentration n_H (a) and mobility μ_H (b) *vs* temperature

As for thermal transport property, the relationship of total thermal conductivity κ with temperature is given in Fig. 7. When Ag_2S is in monoclinic structure, κ is 0.20 $W \cdot m^{-1} \cdot K^{-1}$ at room temperature and is 0.21 $W \cdot m^{-1} \cdot K^{-1}$ near 400 K. Here it is necessary to mention that the thermal conductivity is deduced from the measured thermal diffusion coefficient and then approximately calculated through Dulong-Petit law. Thus, there may be certain errors to the accurate κ of the material. However, the result indicates that the thermal conductivity of α-Ag_2S is indeed ultralow and very stable. In α-Ag_2S, 2 S atoms and 6 Ag atoms form weak chemical bonds along (100) plane. Thus, α-Ag_2S would show low phonon vibration frequency because of the weak binding force of S to Ag[11]. As a result, the low-frequency optical branch dominated by Ag atoms can strongly scatter lattice phonons which have similar frequency. This is the key reason why α-Ag_2S has ultra-low thermal conductivity. When α-Ag_2S turns to β-Ag_2S, κ is quickly increased and keeps steady between 450–600 K and the value is ~0.45 $W \cdot m^{-1} \cdot K^{-1}$. It should be noted that the sulfur element might have slight volatilization during experiment. However, the effect of possible sulfur loss on thermoelectric properties is negligible, as the Ag_2S hardly allows stoichiometric deviation of 2∶1 according to the Ag-S phase diagram. Even though any sulfur loss takes place, the excessive Ag would precipitate on the

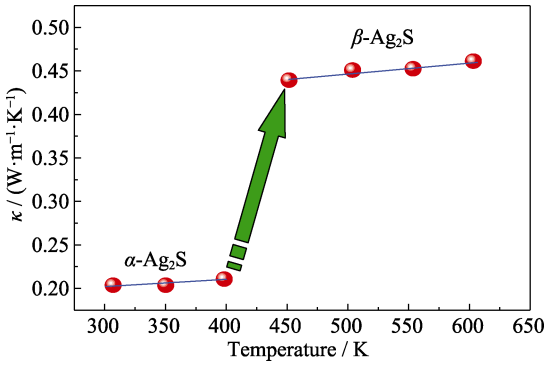

Fig. 7 Relationship between κ and temperature

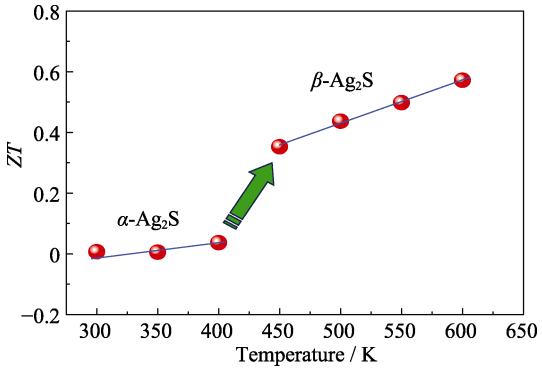

Fig. 8　Dependence of *ZT* with temperature

sample surface to maintain Ag_2S composition stability.

Ultimately, the temperature dependence of *ZT* is displayed in Fig. 8. Due to the extremely weak electrical transport property, α-Ag_2S has very small *ZT* although its thermal transport is quite low. Nevertheless, the *ZT* of β-Ag_2S is about 0.35 at 450 K and reaches 0.57 near 600 K. The present maximum *ZT* is comparable to that of Ag_2S fabricated by melting method (*ZT*=0.55, 580 K)[14], and is on the same level compared with other Ag-based materials, such as Ag_2Se, Ag_2Te, CuAgSe and so on[21-23]. This result verifies that such metal sulfide Ag_2S is a potential low-temperature thermoeletric material. In the future, Ag_2S with element doping is suggested to do help for thermoelectric property improvement.

3　Conclusions

A ϕ18 mm×50 mm Ag_2S ingot was fabricated using zone melting method. It undergoes a phase transition from α-Ag_2S monoclinic $P2_1/c$ space group to β-Ag_2S body centered cubic structure near 450 K, which has remark influence on its electrical and thermal properties. Ag_2S is a *n*-type semiconductor as the Seebeck constant *S* is always negative. The *PF* of α-Ag_2S is much poor because of the weak conductive behavior, but the value would suddenly jump to ~6 $\mu W \cdot cm^{-1} \cdot K^{-2}$ when phase transition happens. The κ of α-Ag_2S and β-Ag_2S are ~0.20 $W \cdot m^{-1} \cdot K^{-1}$ and ~0.45 $W \cdot m^{-1} \cdot K^{-1}$, respectively. Finally, Ag_2S displays a largest *ZT*= 0.57 near 580 K that means it might be a potential middle-temperature TE material.

References:

[1] AlZAHRANI A A, ZAINAL Z, TALIB Z A, *et al*. Study the effect of the heat treatment on the photoelectrochemical performance of binary heterostructured photoanode Ag_2S/ZnO nanorod arrays in photoelectrochemical cells. *Materials Science Forum*, 2020, **1002:** 187–199.

[2] ALHARTHI S S, ALZAHRANI A, RAZVI M A N, *et al*. Spectroscopic and electrical properties of Ag_2S/PVA nanocomposite films for visible-light optoelectronic devices. *Journal of Inorganic and Organometallic Polymers and Materials*, 2020, **30:** 3878–3885.

[3] XIE Y, YOO S H, CHEN C, *et al*. Ag_2S quantum dots-sensitized TiO_2 nanotube array photoelectrodes. *Materials Science and Engineering B*, 2012, **177(1):** 106–111.

[4] KONDRATENKO T S, SMIRNOV M S, OVCHINNIKOV O V, *et al*. Nonlinear optical properties of hybrid associates of Ag_2S quantum dots with erythrosine molecules. *Optik-International Journal for Light and Electron Optics*, 2020, **200:** 163391.

[5] YOU J C, ZHAN S B, WEN J, *et al*. Construction of heterojunction of Ag_2S modified yttrium manganate visible photocatalyst and study on photocatalytic mechanism. *Optik-International Journal for Light and Electron Optics*, 2020, **217:** 164900.

[6] VOGEL R, HOYER P, WELLER H. Quantum-sized PbS, CdS, Ag_2S, Sb_2S_3, and Bi_2S_3 particles as sensitizers for various nanoporous wide-bandgap semiconductors. *The Journal of Physical Chemistry*, 1994, **98(12):** 3183–3188.

[7] DONG Z M, SUN H S, XU J, *et al*. Preparation of macroscopical long Ag_2S nanowire clusters characteristics. *Acta Physica Sinica*, 2011, **60(7):** 676–680.

[8] DU Y P, XU B, FU T, *et al*. Near-infrared photoluminescent Ag_2S quantum dots from a single source precursor. *Journal of the American Chemical Society*, 2010, **132(5):** 1470–1471.

[9] ZHANG Y, HONG G S, ZHANG Y J, *et al*. Ag_2S quantum dot: a bright and biocompatible fluorescent nanoprobe in the second near-infrared window. *ACS Nano*, 2012, **6(5):** 3695–3702.

[10] HWANG I, SEOL M, Kim H, *et al*. Improvement of photocurrent generation of Ag_2S sensitized solar cell through co-sensitization with CdS. *Applied Physics Letters*, 2013, **103(2):** 023902–1–4.

[11] SHI X, CHEN H Y, HAO F, *et al*. Room-temperature ductile inorganic semiconductor. *Nature Materials*, 2018, **17(5):** 421–426.

[12] CHEN Z W, ZHANG X Y, LIN S Q, *et al*. Rationalizing phonon dispersion for lattice thermal conductivity of solids. *National Science Review*, 2018, **5(6):** 888–894.

[13] JEFFREY S G, AGNE M T, RAMYA G. Thermal conductivity of complex materials. *National Science Review*, 2019, **6(3):** 380–381.

[14] WANG T, CHEN H Y, QIU P F, *et al*. Thermoelectric properties of Ag_2S superionic conductor with intrinsically low lattice thermal conductivity. *Acta Physica Sinica*, 2019, **68(9):** 18–26.

[15] CHEN H Y, YUE Z M, REN D D, *et al*. Thermal conductivity during phase transitions. *Advanced Materials*, 2019, **31(6):** 1806518.

[16] LU P, LIU H L, YUAN X, *et al*. Multiformity and fluctuation of Cu ordering in Cu_2Se thermoelectric materials. *Journal of Materials Chemistry A*, 2015, **3(13):** 6901–6908.

[17] ZHANG Y B, WANG Y W, XI L L, *et al*. Electronic structure of antifluorite Cu_2X (X=S, Se, Te) within the modified Becke-Johnson potential plus an on-site Coulomb U. *Journal of Chemical Physics*, 2014, **140(7):** 074702.

[18] JIN M, LIN S Q, LI W, *et al*. Fabrication and thermoelectric properties of single-crystal argyrodite Ag_8SnSe_6. *Chemistry of Materials*, 2019, **31:** 2603–2610.

[19] JIANG J, CHEN L D, BAI S Q, *et al*. Thermoelectric properties of p-type $(Bi_2Te_3)_x(Sb_2Te_3)_{1-x}$ crystals prepared *via* zone melting. *Journal of Crystal Growth*, 2005, **277(1–4):** 258–263.

[20] WANG X, XU J T, LIU G Q, *et al*. Texturing degree boosts thermoelectric performance of silver-doped polycrystalline SnSe. *NPG Asia Materials*, 2017, **9(8):** 426.

[21] WANG X B, QIU P F, ZHANG T S, *et al*. Compound defects and thermoelectric properties in ternary CuAgSe-based materials. *Journal of Materials Chemistry A*, 2015, **3(26):** 13662–13670.

[22] DAY T, DRYMIOTIS F, ZHANG T S, *et al*. Evaluating the potential for high thermoelectric efficiency of silver selenide. *Journal of Materials Chemistry C*, 2013, **1(45):** 7568–7573.

[23] PEI Y Z, HEINZ N A, SNYDER G J. Alloying to increase the band gap for improving thermoelectric properties of Ag_2Te. *Journal of Materials Chemistry*, 2011, **21(45):** 18256–18260.

区熔法制备金属硫化物 Ag_2S 及其热电性能研究

金 敏[1], 白旭东[2], 张如林[1], 周丽娜[1], 李荣斌[1]

(1. 上海电机学院 材料学院, 上海 201306; 2. 上海理工大学 材料科学与工程学院, 上海 200093)

摘 要: 金属硫化物 Ag_2S 具有优异的物理化学性能, 在催化、传感及光电子等领域具有广阔的应用空间。本工作利用一种区熔技术制备了尺寸为 ϕ18 mm×50 mm 的 Ag_2S 并对其潜在热电性能进行了研究。Ag_2S 在 450 K 以下具有标准的 α-Ag_2S 单斜 $P2_1/c$ 结构, 450 K 以上发生相变成为立方 β-Ag_2S 相。Ag_2S 在 300~650 K 范围始终具有负的 Seebeck 系数而呈现 *n* 型半导体特征, 这主要是因为材料中存在 Ag 间隙离子而提供了多余电子。Ag_2S 的 Seebeck 系数在室温下约为−1200 μV·K^{-1}, 440 K 时降为−680 μV·K^{-1}, 当转变为 β-Ag_2S 后则大幅降至~−100 μV·K^{-1}。α-Ag_2S 的电导率几乎为零, 然而在刚发生 β-Ag_2S 相变(450 K)时, 电导率突然增加至~40000.5 S·m^{-1}, 而后随着温度持续升高, 其值在 650 K 降低为 33256.2 S·m^{-1}。霍尔测试表明 Ag_2S 的载流子浓度 n_H 在相变时可从~10^{17} cm^{-3} 迅速增加到~10^{18} cm^{-3} 量级。α-Ag_2S 和 β-Ag_2S 的总热导率 κ 几乎是常数, 分别为~0.20 和~0.45 W·m^{-1}·K^{-1}。最终 Ag_2S 在 580 K 获得最大 *ZT* 值 0.57, 说明它是一种很有发展潜力的中温热电材料。

关 键 词: Ag_2S; 区熔; 热电材料; 相转变

中图分类号: TQ174 **文献标志码**: A